Scientia Iranica D (2021) 28(3), 1661–1668

SCIENTIA IRANICA

Sharif University of Technology
Scientia Iranica
Transactions D: Computer Science & Engineering and Electrical Engineering
http://scientiairanica.sharif.edu

Discontinuous coupling and transition from synchronization to an intermittent transient chimera state

Z. Wang[a], I. Hussain[b], V.-T. Pham[c,d,*], and T. Kapitaniak[d]

a. *Shaanxi Engineering Research Center of Controllable Neutron Source, School of Science, Xijing University, Xi'an 710123, P.R. China.*
b. *Department of Mathematics, Statistics and Physics, Qatar University, Doha 2713, Qatar.*
c. *Nonlinear Systems and Applications, Faculty of Electrical and Electronics Engineering, Ton Duc Thang University, Ho Chi Minh City 758307, Vietnam.*
d. *Division of Dynamics, Lodz University of Technology, Stefanowskiego 1/15, 90-924 Lodz, Poland.*

Received 21 December 2020; received in revised form 12 February 2021; accepted 26 April 2021

KEYWORDS
Synchronization;
Chimera state;
Chaos;
Coupled oscillators;
Discontinuous coupling.

Abstract. Coexistence of coherent and incoherent clusters, called chimera state, has been observed in different coupling configurations. A majority of studies have considered a static scheme for the network. In this paper, synchronization patterns of a time-varying network with discontinuous coupling (on/off links) were studied. At first, the prerequisites for synchronization of continuous and discontinuous coupling were found using the master stability function method. It was observed that when the network with continuous coupling was set in the synchronous region, changing the coupling to a discontinuous one would lead to the emergence of a pattern consisting of alternating synchronization, asynchronization, and chimera state. This pattern is called intermittent transient chimera here. This study is completed by investigating the effect of the rate of discontinuity on the network behavior.

1. Introduction

Synchronization is a ubiquitous event in nature that has many applications in different sciences, ranging from physics to technology and society [1]. Recently, a majority of the studies have focused on the synchronous states in the network of coupled oscillators [2,3]. Relevant surveys have demonstrated different synchronous patterns such as explosive synchronization, generalized synchronization, partial synchronization, coexistence of synchronization and asynchronization, etc. [1,4,5]. Chimera state is a special spatiotemporal pattern in the networks, wherein there exist both groups of coherent and incoherent oscillators [6,7].

The initial survey of the chimera state belonged to a network of non-locally coupled complex Ginzburg-Landau oscillators [8]. This state has drawn considerable attention after its discovery in different fields such as mechanics and biology [9–18]. In addition, several experimental investigations have reported the appearance of chimera states in optical [19], chemical [20,21], mechanical [22–24], and electronic systems [25]. Chimera state has certain associations with numerous real events. The most relevant one is the uni-hemispheric sleep, during which half part of the brain is asleep and synchronous, and the other is awake and asynchronized. Other related events are brain disor-

*. *Corresponding author.*
E-mail address: phamvietthanh@tdtu.edu.vn (V.-T. Pham)

doi: 10.24200/sci.2021.57386.5212

ders including Epileptic seizures, Parkinson's disease, Alzheimer's disease, etc. [26]. Due to this relevance, the chimera states have been studied in different neuronal networks [27–30]. Recently, a comprehensive review of chimera states in neuronal networks was proposed by Majhi et al. [26]. Bansal et al. [31] studied the emergence of chimera state in an empirical neuronal network with 76 brain regions. They considered nine cognitive systems and found that the chimera state was linked to cognitive brain functions.

Initially, the chimera state was reported in a non-local coupling scheme [8]. Then, the studies indicated that chimeras could also appear in networks with local or global connections [32,33]. For example, Clerc et al. [34] investigated the emergence, stability properties, and bifurcation diagram of chimera-like states in a locally coupled network and found the required conditions necessary for their emergence. If the oscillators are globally coupled, it is expected that they have similar motions in time [33]. Schmidt and Krischer [35] considered a globally coupled network and searched for the necessities for the emergence of the chimera state. They reported that the first requisite was a clustering mechanism for splitting the oscillators into two groups. Among the studies, a few ones considered time-varying coupling [36–39]. For instance, Buscarino et al. [36] investigated a two population network of coupled Kuramoto oscillators with time-varying links. They found that diverse patterns of chimeras such as stable, breathing, and alternating chimera states could emerge in this network. The adaptive coupling was also studied in the globally coupled Kuramoto-type oscillators [37]. It was found that the formed synchronous clusters depended on the adaptation function. Huo et al. [39] considered adaptive coupling in the network of FitzHugh-Nagumo models with three different structures including the global, random, and scale-free ones. This study revealed that adaptive coupling played a key role in the occurrence of chimera; however, it has different evolutions in three structures.

In this paper, the effect of discontinuous coupling on the synchronization behavior of the network was studied. It was assumed that the links were on at a time interval and then, off at the next time interval. At first, the prerequisites for the synchronization of the continuous and discontinuous couplings were found using the Master Stability Function (MSF). Then, the network was numerically solved, and it was observed that by adjusting the coupling discontinuously, the behavior of the network changed from the complete to an intermittent synchronous state, in which the behavior of the network changed alternatively between synchronization and asynchronization. During this alternation, the chimera state was observed. Therefore, the pattern intermittent was referred to as the transient chimera in this study. Finally, the effect of the on/off rate on the network behavior was studied.

2. The model

Lorenz system was selected for the elements of our network. Figure 1 shows the time series and phase space of the Lorenz system. The equations of the ith node of the network can be described as follows:

$$\dot{x}_i = s(y_i - x_i) + \varepsilon \sum_{j=1}^{N} G_{ij} x_j,$$

$$\dot{y}_i = x_i(\rho - z_i) - y_i, \qquad \dot{z}_i = x_i y_i - \beta z_i, \tag{1}$$

where $N = 100$ indicates the number of the nodes in the network, ε is the coupling strength, G_{ij} is the zero-row sum coupling matrix with $G_{ij} = 1$, if node i and j are connected, and:

$$G_{ij} = 0 \text{ else, and}: \; G_{ii} = -\sum_{j=1, j\neq i}^{N} G_{ij}.$$

The parameters are $\rho = 28$, $s = 10$, and $\beta = 2$. A restriction was put on the matrix G so that at a time interval $nT < t < (n+\theta)T$, all the connections were on with $G_{ij} = 1$, $i,j = 1,...,N$, $i \neq j$ and at the

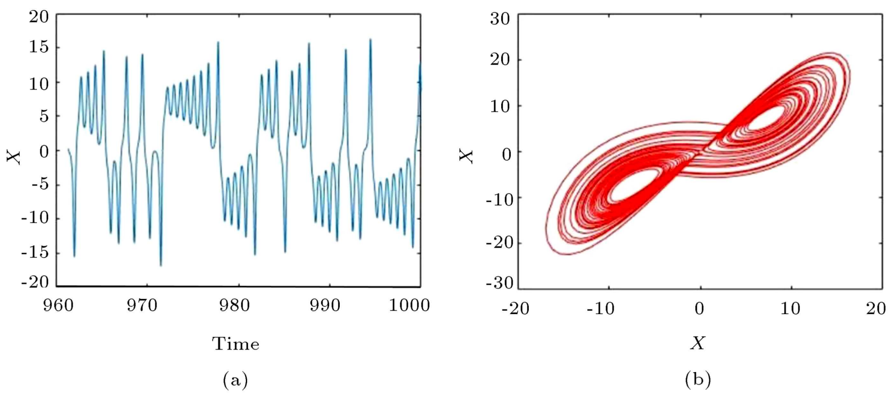

Figure 1. Time series (a) and phase portrait (b) of the Lorenz system.

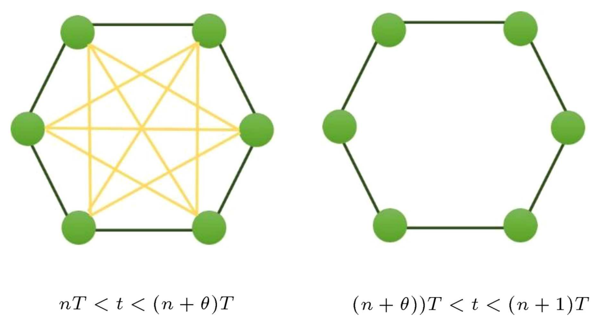

Figure 2. The schematic of the network with discontinuous coupling for $N = 6$ nodes.

next time interval $(n+\theta)T < t < (n+1)T$, all the connections except the nearest neighbors were off, i.e., $G_{ij} = 1$, $j = i+1$, $i-1$. This process was repeated periodically and θ was called the discontinuity rate, $0 < \theta < 1$. Figure 2 represents the schematic of the described network with $N = 6$ nodes.

To evaluate the coherence of the oscillators, the local order parameter was applied. This measure that specifies the local ordering of the network units is calculated as follows [26]:

$$L_i = \left| \frac{1}{2v} \sum_{|i-k| \leq v} e^{j\Phi_k} \right|, \qquad i = 1, ..., N, \tag{2}$$

where $j = \sqrt{-1}$ and $v = 3$ is the number of the nearest neighbors, and Φ_i is the geometric phase of the ith oscillator. In addition, the geometric phase was calculated as $\Phi_i = \arctan(\frac{y_i}{x_i})$ [40–42]. The local order parameter determines whether or not a unit belongs to a coherent group. In fact, $L_i = 1$ represents belonging to a coherent group, while $L_i = 0$ shows that the ith unit belongs to an incoherent group.

3. Results

The above network is firstly considered in the case of continuous coupling, i.e., $G_{ij} = 1$, $i, j = 1, ..., N$, $i \neq j$ for all t. MSF method is an analytical approach to finding sufficient conditions for synchronization of a network [43]. To calculate MSF, firstly, the variational equations should be obtained which is as follows:

$$\xi_k = [DF + \varepsilon\gamma_k DH]\xi_k, \tag{3}$$

where F is the equations of the uncoupled system (here, Lorenz system), D the Jacobean, and H the coupling function, which is defined here as:

$$H = DH = \begin{bmatrix} 1 & 0 & 0 \\ 0 & 0 & 0 \\ 0 & 0 & 0 \end{bmatrix},$$

since the coupling is between x variables. Moreover, γ_k, $k = 0, 1, ..., N$ are the eigenvalues of the coupling matrix (G). Since the network is connected, the eigenvalues of G have the property of $\gamma_1 = 0 < \gamma_2 < ... < \gamma_N$. The largest Lyapunov exponent of the variational equations (Eq. (3)) is the MSF that determines the stability of the synchronous state. Usually, MSF is computed considering that $K = \varepsilon\gamma_k$ and the MSF< 0 shows that the synchronous state is stable. Given that the zero-crossing point of MSF is $K = \varepsilon\gamma_k$, the smallest γ_k results in the higher coupling strength (ε) needed for stable synchronization. Therefore, in our investigations, we have only considered γ_2 to obtain the ε larger, which ensures the synchronization.

For the continuous network of Eq. (1), the variational equations are as follows:

$$\dot{\xi}_1 = (-(\varepsilon\gamma) - s)\xi_1 + s\xi_2,$$
$$\dot{\xi}_2 = (\rho - z)\xi_1 - \xi_2 - x\xi_3,$$
$$\dot{\xi}_3 = y\xi_1 + x\xi_2 - \beta\xi_3. \tag{4}$$

The largest Lyapunov exponent of Eq. (4), which is the MSF of the continuous network, is shown in Figure 3 in black color. According to this curve, the network is synchronous for $\varepsilon > 0.076$.

By assuming the links to be discontinuous, the coupling strength threshold at which the network is synchronous would change. In this case, the coupling matrix (G) and its eigenvalues are time-varying. Hence, the variational equations of the discontinuous network can be given as follows:

$$\dot{\xi}_1 = (-(\varepsilon\gamma(t)) - s)\xi_1 + s\xi_2,$$
$$\dot{\xi}_2 = (\rho - z)\xi_1 - \xi_2 - x\xi_3,$$
$$\dot{\xi}_3 = y\xi_1 + x\xi_2 - \beta\xi_3, \tag{5}$$

where $\gamma(t)$ switches between two eigenvalues of the global coupling matrix (for $\Delta t = \frac{\theta}{T}$) and local coupling matrix (for $\Delta t = \frac{1-\theta}{T}$). In this study, the largest

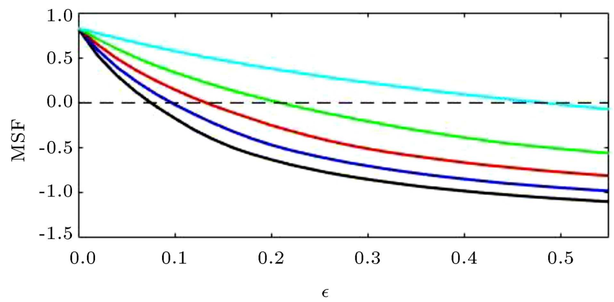

Figure 3. Master Stability Function (MSF) of the continuous network (black) and the discontinuous network for $T = 0.1$ and different rates with respect to coupling strength. The curves of $\theta = 0.8, 0.6, 0.4, 0.2$ are shown by blue, red, green, and cyan, respectively.

Lyapunov exponents of the variational equation (Eq. (5)) were calculated versus the coupling strength. The period of discontinuity was set at $T = 0.1$. The results are shown in Figure 3 for $\theta = 0.2, 0.4, 0.6, 0.8$. According to this figure, as the discontinuity rate decreases, the synchronization state becomes stable in higher coupling strength values. These results are very close to (not exactly the same) the numerical solutions of the network.

For further investigations, this study evaluated the effects of the period of discontinuity on the synchronization threshold obtained by the largest Lyapunov exponent of the time-varying variational equations (Eq. (5)). To this end, two discontinuity rates of $\theta = 0.4$ and 0.6 were taken into account and the MSF of the time-averaged network was computed. Then, the largest Lyapunov exponent of Eq. (5) was calculated by setting the discontinuity period at $T = 0.05, 0.1, 0.5, 1$, the results of which are presented in Figure 4. As observed, for very short discontinuity periods, the solutions of the time-varying equations were quite close to those of the time-averaged one. As the discontinuity period increased, the synchrony threshold moved farther away. Moreover, it seems that the value of period T has a greater effect on the lower θ values.

For numerical simulations of the discontinuous network, the fourth-order Runge-Kutta method with the time step of 0.01 was used. The initial conditions of the oscillators were randomly selected. The coupling strength value was chosen to be $\varepsilon = 0.1$ at which the continuous network was synchronous. To confirm this, Figure 5 shows the space-time plot and time snapshot of the network for this coupling strength. Figure 6 illustrates the space-time plot and snapshot of the network, assuming equal time intervals for the discontinuity process, i.e., $\theta = 0.5$. According to this figure, when coupling becomes discontinuous, the network synchronization is disturbed and some incoherent regions are detected in the space-time plot. In fact, the time evolution of the network represents an alternation between synchronization and asynchronization in time.

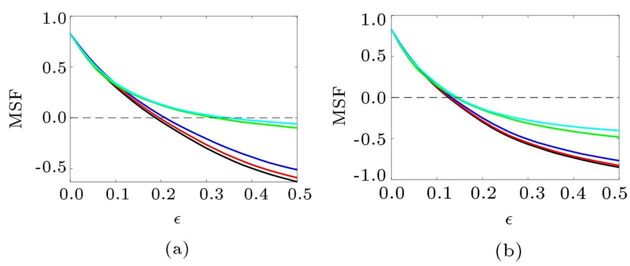

Figure 4. Master Stability Function (MSF) of the averaged network (shown in black) and the Largest Lyapunov Exponent (LLE) of the variational equation (Eq. (5)) for $T = 0.05, 0.1, 0.5, 1$ (shown in red, blue, green, and cyan): (a) $\theta = 0.4$ and (b) $\theta = 0.6$.

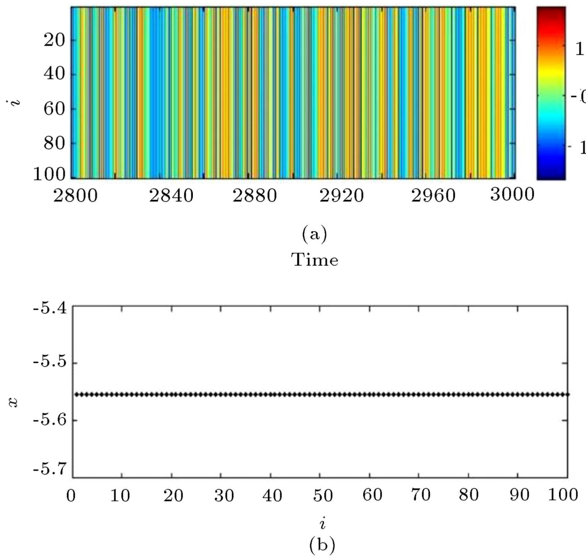

Figure 5. The synchronous patterns for continuous coupling with $\varepsilon = 0.1$: (a) Space-time plot and (b) time snapshot.

In these transitions from synchrony to asynchrony at short time intervals, the coexistence of synchronous and asynchronous domains can be observed. The formation of the synchronous and asynchronous regions can be referred to as the chimera state; however, since this coexistence occurs alternatively at short time intervals, the observed pattern is referred to as an intermittent transient chimera in this study. The local order parameter of the network, in this case, is demonstrated in Figure 6(b) that confirms the existence of intermittent synchronization, chimera, and asynchronization. The time snapshots of the network at different times are presented in Figure 6(c). Figure 7 demonstrates the time series of the first and second oscillators. Based on the time series, it can be concluded that these two oscillators are only synchronous at a time interval and then, they become asynchronous again.

In the next step, the network patterns are investigated by varying the discontinuity rate (θ). Figure 8 illustrates the pattern of the network for different θ values. In Figure 8(a), the network pattern with $\theta = 0.8$ is plotted which shows the synchronization state. Thus, the discontinuous coupling with a low rate cannot change the synchronized behavior of the oscillators. Figure 8(b) and (c) show the network behavior for $\theta = 0.6, 0.4$, respectively, at which the synchronous state of the network is disturbed, and the incoherent regions appear in the network. In case the discontinuity rate is set to lower values, the synchronous state is completely destroyed and the oscillators oscillate asynchronously. Figure 8(d) shows the asynchronous state for $\theta = 0.2$.

To completely survey the network behavior, a phase diagram in (θ, ε) plane is provided in Figure 9.

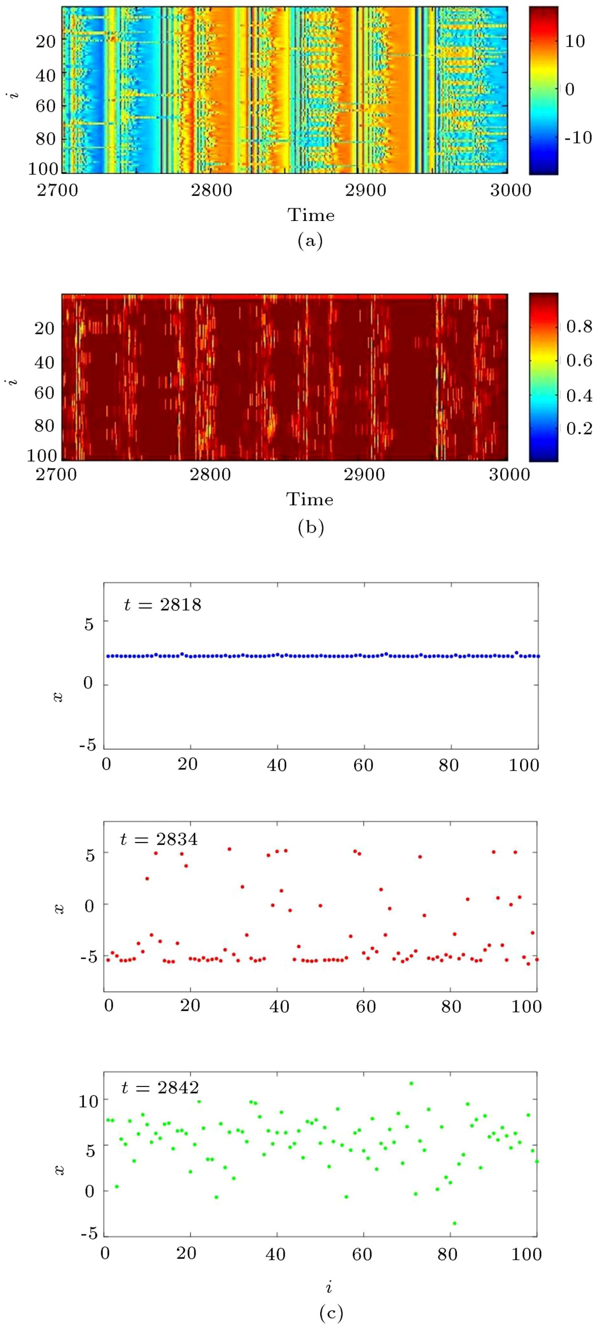

Figure 6. The network patterns for discontinuous coupling with $\theta = 0.5$ and $\varepsilon = 0.1$: (a) space-time plot, (b) local order parameter, and (c) time snapshots at $t = 2818$ (synchronized behavior), $t = 2834$ (chimera state) and $t = 2842$ (asynchronized behavior).

In this figure, the synchronous state is shown in green, the intermittent transient chimera state in yellow, and asynchronous state in red. According to this diagram, as the discontinuity rate (θ) grows, the asynchronous state region and the chimera region are reduced and the network tends to become synchronous, even for smaller coupling strengths.

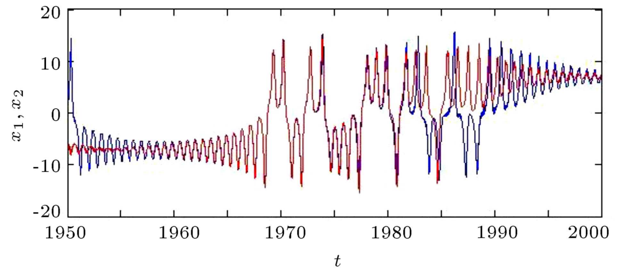

Figure 7. Time series of the first and second oscillators of the network with discontinuous coupling for $\theta = 0.5$ and $\varepsilon = 0.1$.

4. Conclusion

The present study mainly focused on the consequences of discontinuous coupling on the synchronous motion of the network. Firstly, the network was considered with continuous global coupling and the coupling strength threshold, leading to the synchronous state, was obtained using the Master Stability Function (MSF) method. Then, the coupling was assumed to be discontinuous, switching between the global and local coupling at different rates. To evaluate the effect of the discontinuous links on the synchronization threshold, MSF method was modified using the time-dependent eigenvalues in the variational equations. Then, the largest Lyapunov exponents of the new variational equations were calculated at different discontinuity rates. The results indicated that a higher coupling strength was needed for synchronization of the network with on/off links. Moreover, upon decreasing the discontinuity rate (i.e., on to off rate), this threshold increased. The synchrony threshold obtained from the time-dependent variational equations was quite close to that found through numerical solutions, yet not exactly the same. The effect of the discontinuity period on the synchronization results was evaluated by computing the MSF of the network in the case of time-averaged coupling matrix and time-varying one in different periods. It was found that for small periods, the values of the time-averaged and time-varying MSF curves were quite close; however, upon lengthening the period, they would become quite distant.

Numerical simulations of the network showed that discontinuing the coupling shifted the network behavior from complete synchronization to an alternation between synchronization and asynchronization states. During this transition from synchrony to asynchrony, the chimera state emerged. Since this chimera state was transient and alternately repeated over time, it was referred to as the intermittent transient chimera in this study. To evaluate the coherence of the network, the local order parameter was used. The simulations were done at different discontinuity rates and a phase diagram of the network behavior was presented.

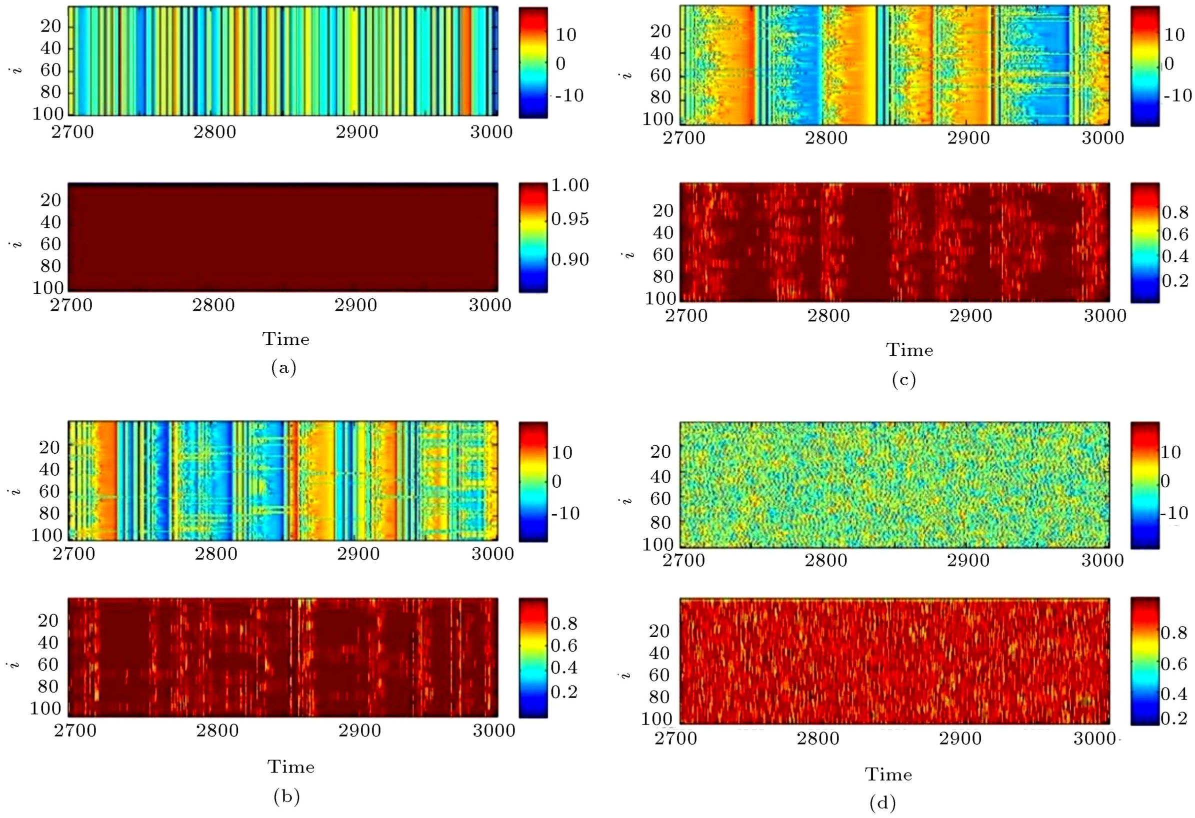

Figure 8. The network patterns (upper figure: space-time plot; lower figure: local order parameter) for discontinuous coupling with $\varepsilon = 0.1$ for (a) $\theta = 0.8$, (b) $\theta = 0.6$, (c) $\theta = 0.4$, and (d) $\theta = 0.2$.

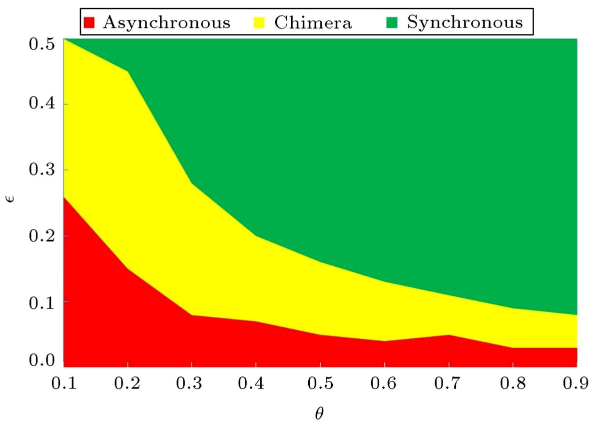

Figure 9. Phase diagram of the network in (θ, ε) plane.

Acknowledgement

Z W was supported by the Natural Science Basic Research Plan in Shaanxi Province of China (2020JM-646), the Innovation Capability Support Program of Shaanxi (2018GHJD-21), and Science and Technology Program of Xi'an (2019218414GXRC020CG021-GXYD20.3). T K was supported by the National Science Centre, Poland, MAESTRO Programme-Project No. 2013/08/A/ST8/00780, and OPUS Programme-2018/29/B/ST8/00457.

References

1. Boccaletti, S., Kurths, J., Osipov, G., et al. "The synchronization of chaotic systems", *Phys. Rep.*, **366**(1–2), pp. 1–101 (2002).
2. Majhi, S. and Ghosh, D. "Synchronization of moving oscillators in three dimensional space", *Chaos*, **27**(5), p. 053115 (2017).
3. Pecora, L.M. and Carroll, T.L. "Synchronization of chaotic systems", *Chaos*, **25**(9), p. 097611 (2015).
4. Zhang, X., Boccaletti, S., Guan, S., et al. "Explosive synchronization in adaptive and multilayer networks", *Phys. Rev. Lett.*, **114**(3), p. 038701 (2015).
5. Panaggio, M.J. and Abrams, D. M. "Chimera states: coexistence of coherence and incoherence in networks of coupled oscillators", *Nonlinearity*, **28**(3), p. R67 (2015).
6. Abrams, D.M., Strogatz, S.H., et al. "Chimera states for coupled oscillators", *Phys. Rev. Lett.*, **93**(17), p. 174102 (2004).
7. Parastesh, F., Jafari, S., Azarnoush, H., et al. "Chimeras", *Phys. Rep.*, (2020) (In Press).
8. Kuramoto, Y. and Battogtokh, D. "Coexistence of coherence and incoherence in nonlocally coupled phase oscillators", *Nonl. Phen. Compl. Syst.*, **5**(4), pp. 380–385 (2002).

9. Majhi, S., Perc, M., and Ghosh, D. "Chimera states in a multilayer network of coupled and uncoupled neurons", *Chaos*, **27**(7), p. 073109 (2017).

10. Omelchenko, I., Provata, A., Hizanidis, J., et al. "Robustness of chimera states for coupled FitzHugh-Nagumo oscillators", *Phys. Rev. E.*, **91**(2), p. 022917 (2015).

11. Wei, Z., Parastesh, F., Azarnoush, et al. "Nonstationary chimeras in a neuronal network", *EPL (Europhys. Lett.)*, **123**(4), p. 48003 (2018).

12. Chouzouris, T., Omelchenko, I., Zakharova, et al. "Chimera states in brain networks: Empirical neural vs. modular fractal connectivity", *Chaos*, **28**(4), p. 045112 (2018).

13. Loos, S.A., Claussen, J.C., Schöll, E., et al. "Chimera patterns under the impact of noise", *Phys. Rev. E.*, **93**(1), p. 012209 (2016).

14. Dudkowski, D., Maistrenko, Y., and Kapitaniak, T. "Occurrence and stability of chimera states in coupled externally excited oscillators", *Chaos*, **26**(11), p. 116306 (2016).

15. Parastesh, F., Chen, C.-Y., Azarnoush, H., et al. "Synchronization patterns in a blinking multilayer neuronal network", *Eur. Phys. J. Spec. Top.*, **228**(11), pp. 2465–2474 (2019).

16. Wang, Z., Baruni, S., Parastesh, et al. "Chimeras in an adaptive neuronal network with burst-timing-dependent plasticity", *Neurocomputing*, **406**, pp. 117–126 (2020).

17. Parastesh, F., Jafari, S., Azarnoush, H., et al. "Chimera in a network of memristor-based Hopfield neural network", *Eur. Phys. J. Spec. Top.*, **228**(10), pp. 2023–2033 (2019).

18. Khaleghi, L., Panahi, S., Chowdhury, S.N., et al. "Chimera states in a ring of map-based neurons", *Physica A.*, **536**, p. 122596 (2019).

19. Hagerstrom, A.M., Murphy, T.E., Roy, R., et al. "Experimental observation of chimeras in coupled-map lattices", *Nature Phys.*, **8**(9), p. 658 (2012).

20. Nkomo, S., Tinsley, M.R., and Showalter, K., "Chimera states in populations of nonlocally coupled chemical oscillators", *Phys. Rev. Lett.*, **110**(24), p. 244102 (2013).

21. Awal, N.M., Bullara, D., and Epstein, I.R. "The smallest chimera: Periodicity and chaos in a pair of coupled chemical oscillators", *Chaos*, **29**(1), p. 013131 (2019).

22. Dudkowski, D., Grabski, J., Wojewoda, J., et al. "Experimental multistable states for small network of coupled pendula", *Sci. Rep.*, **6**, p. 29833 (2016).

23. Dudkowski, D., Czołczyński, K., and Kapitaniak, T. "Traveling chimera states for coupled pendula", *Nonlinear Dyn.*, **95**(3), pp. 1859–1866 (2019).

24. Carvalho, P.R. and Savi, M.A. "Synchronization and chimera state in a mechanical system", *Nonlinear Dyn.*, pp. 1–19 (2020).

25. Gambuzza, L.V., Buscarino, A., Chessari, S., et al. "Experimental investigation of chimera states with quiescent and synchronous domains in coupled electronic oscillators", *Phys. Rev. E.*, **90**(3), p. 032905 (2014).

26. Majhi, S., Bera, B.K., Ghosh, D., et al. "Chimera states in neuronal networks: A review", *Phys. Life Rev.*, **28**, pp. 100–121 (2019).

27. Bao, H., Zhang, Y., Liu, W., et al. "Memristor synapse-coupled memristive neuron network: synchronization transition and occurrence of chimera", *Nonlinear Dyn.*, **100**, pp. 937–950 (2020).

28. Andreev, A.V., Ivanchenko, M.V., Pisarchik, A.N., et al. "Stimulus classification using chimera-like states in a spiking neural network", *Chaos, Solitons & Fractals*, **139**, p. 110061 (2020).

29. Wang, S., He, S., Rajagopal, K., et al. "Route to hyperchaos and chimera states in a network of modified Hindmarsh-Rose neuron model with electromagnetic flux and external excitation", *Euro. Phys. J. Spec. Top.*, **229**, pp. 929–942 (2020).

30. Ruzzene, G., Omelchenko, I., Sawicki, J., et al. "Remote pacemaker control of chimera states in multilayer networks of neurons", *Phys. Rev. E.*, **102**(5), p. 052216 (2020).

31. Bansal, K., Garcia, J.O., Tompson, S.H., et al. "Cognitive chimera states in human brain networks", *Sci. Adv.*, **5**(4), p. eaau8535 (2019).

32. Bera, B.K. and Ghosh, D. "Chimera states in purely local delay-coupled oscillators", *Phys. Rev. E.*, **93**(5), p. 052223 (2016).

33. Yeldesbay, A., Pikovsky, A., and Rosenblum, M. "Chimeralike states in an ensemble of globally coupled oscillators", *Phys. Rev. Lett.*, **112**(14), p. 144103 (2014).

34. Clerc, M., Coulibaly, S., Ferré, M., et al. "Chimera-type states induced by local coupling", *Phys. Rev. E.*, **93**(5), p. 052204 (2016).

35. Schmidt, L. and Krischer, K. "Clustering as a prerequisite for chimera states in globally coupled systems", *Phys. Rev. Lett.*, **114**(3), p. 034101 (2015).

36. Buscarino, A., Frasca, M., Gambuzza, L.V., et al. "Chimera states in time-varying complex networks", *Phys. Rev. E.*, **91**(2), p. 022817 (2015).

37. Kasatkin, D., Yanchuk, S., Schöll, E., et al. "Self-organized emergence of multilayer structure and chimera states in dynamical networks with adaptive couplings", *Phys. Rev. E.*, **96**(6), p. 062211 (2017).

38. Kasatkin, D. and Nekorkin, V. "Synchronization of chimera states in a multiplex system of phase oscillators with adaptive couplings", *Chaos*, **28**(9), p. 093115 (2018).

39. Huo, S., Tian, C., Kang, L., et al. "Chimera states of neuron networks with adaptive coupling", *Nonlinear Dyn.*, **96**(1), pp. 75–86 (2019).

40. Bera, B.K., Ghosh, D., and Banerjee, T. "Imperfect traveling chimera states induced by local synaptic gradient coupling", *Phys. Rev. E.*, **94**(1), p. 012215 (2016).

41. Omelchenko, I., Omel'chenko, E., H;vel, P., et al. "When nonlocal coupling between oscillators becomes stronger: patched synchrony or multichimera states", *Phys. Rev. Lett.*, **110**(22), p. 224101 (2013).

42. Kundu, S., Bera, B.K., Ghosh, D., et al. "Chimera patterns in three-dimensional locally coupled systems", *Phys. Rev. E.*, **99**(2), p. 022204 (2019).

43. Pecora, L.M. and Carroll, T.L. "Master stability functions for synchronized coupled systems", *Phys. Rev. Lett.*, **80**(10), p. 2109 (1998).

Biographies

Zhen Wang was born in Shaanxi, China in 1981. He received his BSc and MSc degrees in 2004 and 2008, respectively, from Shaanxi University of Science and Technology, China. He is currently a Professor at School of Science at Xijing University. His research interests include ordinary differential equations and dynamical systems, nonlinear control system theory, etc.

Iqtadar Hussain is an Assistant Professor at Qatar University. He received his PhD in Mathematics in 2014, specializing in the area of Cryptography. His current research expertise and research interests include applications of mathematical concepts in the field of secure communication and cybersecurity where he has published 80 papers in well-known journals. His h-index score is 25 and i-10 index score is 42. His articles have 1660 Google Scholar citations.

Viet-Thanh Pham received the PhD degree in Electronics, Automation, and Control of Complex Systems Engineering. His scientific interests include applications of nonlinear systems, chaos, analysis and design of analog circuits, and FPGA-based digital circuits.

Tomasz Kapitaniak is a Professor of Nonlinear Dynamics at Lodz University of Technology. He is a Corresponding Member of the Polish Academy of Sciences. His research interests include mechanical oscillations, nonlinear systems, stability, bifurcations and chaos, stochastic dynamics, mathematical modeling, ordinary differential equations, vibro-impact systems, and applications of nonlinear dynamics in mechanical engineering.